Structural model of the mitral valve included in a cardiovascular closed loop model Static and dynamic validation

S. Paeme*, K. Moorhead*, JG. Chase, CE. Hann**, B. Lambermont*, P. Kolh*, M. Moonen*, P. Lancellotti*, P.C. Dauby*, T. Desaive***

** Cardiovascular Research Center, University of Liege, Liege, Belgium*
*** Department of Mechanical Engineering, University of Canterbury, Christchurch, New Zealand*

Abstract: A minimal cardiovascular system (CVS) model including mitral valve dynamics has been previously validated *in silico*. It accounts for valve dynamics using a second order differential equation to simulate the physiological opening valve law. This second order equation is based on output heart signals and is really difficult to bind with anatomical or physiological parameters, making this model difficult to interpret and to particularise to pathological situations.

On the other hand, a simple non-linear rotational spring model implemented to model the motion of mitral valve, located between the left atrium and ventricle has been validated on a literature dataset. A measured pressure difference curve was used as the input into the model, which represents an applied torque to the valve chords. Various damping and hysteresis states were investigated to find a model that best matches reported animal data of chord movement during a heartbeat. This model is based on simple physiological behavior modeling, defining parameters linked with physiological or anatomical data.

This research describes a new closed-loop CVS model corresponding to the integration of the simple non-linear rotational spring model to describe the progressive aperture of the mitral valve in the minimal cardiovascular system closed loop model.

This new model is proved to fit static and dynamic heart behaviour.

Keywords: cardiovascular system model, valve dynamics, mitral valve, cardiac cycle

1. INTRODUCTION

Mathematical models of the cardiovascular system (CVS) vary significantly in their complexity and their objectives. They range from the simple Windkessel model [1] to very complex network representations of the vascular tree [2] and finite element models of several million degrees of freedom [3, 4].

The aim of this research is to improve a "minimal cardiac model" of the CVS [5] changing the way to model mitral cardiac valve. This model was first developed and optimized [5, 6] to assist health professionals in selecting reliable and appropriate therapies. This model is based on the "pressure-volume" (PV) lumped element approach. It divides the cardiovascular system in several chambers described by their own PV relationship [5, 7]. This method requires a limited number of parameters, allowing for easy and rapid simulations and for patient specific identification of disease state at the bedside [8, 9].

Improving the Heaviside formulation of cardiac valves law used in the minimal cardiovascular system (CVS) model has already be done previously [10, 11]. This model accounts for valve dynamics using a second order differential equation to simulate the physiological opening valve law. However, this second order equation is based on output heart signals and is really difficult to bind with anatomical or physiological parameters, making this model difficult to interpret and to particularise to pathological situations.

This research focuses on improving the minimal CVS with a simple cardiac valve model to obtain a CVS model which better fits the reality and which remain easy to interpret and to particularise to pathological situations.

The cardiac valve model used is therefore a simple non-linear rotational spring model implemented to model the motion of mitral valve, located between the left atrium and ventricle has been validated on a literature dataset. A measured pressure difference curve was used as the input into the model, which represents an applied torque to the valve chords. This model is based on simple physiological behavior modeling, defining parameters linked with physiological or anatomical data [12].

This research describes therefore a new closed-loop CVS model corresponding to the integration of the simple non-linear rotational spring model to describe the progressive aperture of the mitral valve in the minimal cardiovascular system closed loop model. This new model will then be proved to fit static and dynamic heart behaviour.

This work was supported by the F.R.I.A. (Belgium), the University of Canterbury and the French Community of Belgium (Actions de Recherches Concertées Académie Wallonie-Europe)

2. METHODS

2.1 The cardiovascular system model (CVS)

We used a CVS model with seven elastic chambers which are the left and right ventricles, the vena cava, the aorta, the pulmonary artery and veins (Figure 1). This model was first described by Smith et al [5] and has already been validated *in silico* and in several animal model studies [8, 10, 13-16]. In Figure 1, resistances (R), inductors (L) and diodes respectively model the resistance of the flows through the arteries, the effects of inertia, and the cardiac valves.

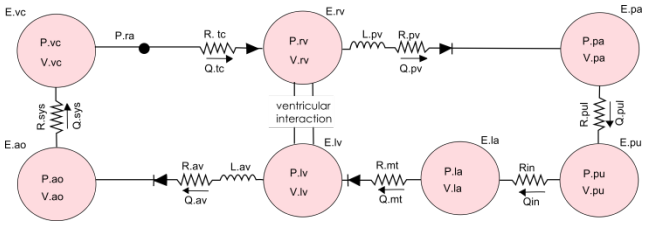

Figure 1 : CVS model made up of 7 elastic chambers and 4 "open on pressure close on flow" law valves

The cardiac chambers are modeled using pressure-volume (PV) relationships. To account for myocardial activation, a time-varying elastance driving function is used over a single heart beat and is defined:

$$e(t) = e^{-80(t-0,27)^2} \quad (1)$$

There are three differential equations describing the rate of change of the cardiac chamber volume and the inflow (Q_{in}) and outflow (Q_{out}) for each chamber:

$$\frac{dV}{dt} = Q_{in} - Q_{out} \quad (2)$$

$$\frac{dQ_{in}}{dt} = \frac{P_{up} - P - Q_{in}R_{in}}{L_{in}} \quad (3)$$

$$\frac{dQ_{out}}{dt} = \frac{P - P_{down} - Q_{out}R_{out}}{L_{out}} \quad (4)$$

where Pup, Pdown and P are the upstream, the downstream and the chamber pressures, Lout and Lin respectively the outer and inner inductors, and Rout and Rin the outer and inner resistances. These equations are valid for the seven chambers of our model.

Ventricular interaction and valve dynamics

Both the septum and the pericardium play major roles in ventricular interaction as they link the two chambers directly. To define the septum volume Vspt we introduce the free wall volumes Vlvf and Vrvf which are not exactly physical volumes. They are defined in Figure 2.

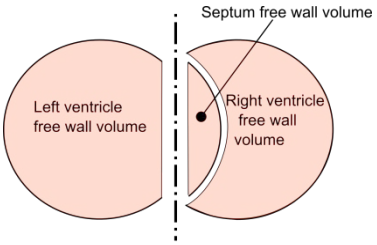

Figure 2 : definition of free wall volumes

Finally, the minimal CVS model assumes that the 4 cardiac valves only exist in two different states: open or closed [5]. Thus, a special procedure is used [6] that automatically accounts for the valves opening and closing, instead of using an event solver to detect when the valve should open or close. This procedure is based on the Heaviside formulation in Equation and minimises computation and computational instability [6].

$$H(x) = \begin{cases} 0 & if \quad x \leq 0 \\ 1 & if \quad x > 0 \end{cases} \quad (5)$$

For each valve, the argument of the Heaviside function is chosen to fulfil the law: “open on pressure, close on flow” [5, 6].

2.2 The mitral valve model

The main drawback of the Heaviside formulation is that it does not take into account physiological time scale of the valve aperture [17]. Therefore, the initial minimal CVS model is not able to fully capture valve dysfunctions. Given the common occurrence of valve dysfunction, it has important clinical implications.

Other valvular models previously studied are either too complex to lead to a complete description of the cardiovascular system easy to interpret either too simple and can’t be used to study pathological situations.

This research uses simple dynamic model of the stiffness of the valve leaflets to characterize the fundamental effects on flow and pressure. The valve is treated as a non-linear rotational spring or a ‘hinge’ with the change in angle under pressure driven flow being related to the stiffness and damping of the valve [12].

$$c\dot{\theta} + F_K(\theta) = \alpha\Delta P \quad (6)$$

where θ is the valve opening angle, c is the damping coefficient due to the blood surrounding the leaflets, $F_K(\theta)$ is the non-linear restoring force, ΔP is the transmitral pressure, and α is a torque constant converting differential pressure into an input torque on the valve.

2.3 Coupling both models

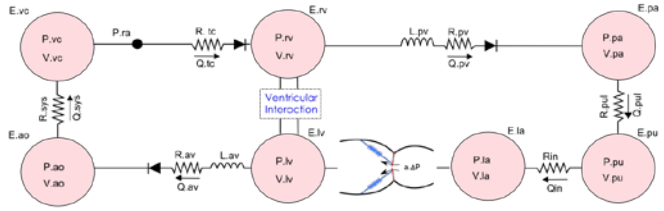

Figure 3 : CVS model made up of 7 elastic chambers and the non-linear rotational spring model of the mitral valve

Based on the expression of the resistance in a cylindrical flow, the mitral resistance is modified to be a function of the mitral aperture:

$$R_{mt} = \frac{8\pi\mu l}{A(t)^2} \tag{7}$$

In the same way, we adapt the expression of the inertance:

$$L_{mt} = \frac{\rho l}{A(t)} \tag{8}$$

The variation of the mitral flow qmt is also updated to take into account the variation of the mitral aperture:

$$\dot{Q_{mt}} = \frac{P_{pu} - P_{lv}}{L_{mt}} - Q_{mt}\frac{R_{mt}}{L_{mt}} + Q_{mt}\frac{\dot{A(t)}}{A(t)} \tag{9}$$

Thus this approach introduces the mitral valve opening area A which is related to the new state variable, θ, the opening mitral valve angle. The mitral valve cross section is supposed to be circular so that:

$$A = \pi r^2(1 - \cos\theta)^2 \tag{10}$$

where r is the mitral cross section radius.

We simulate the model (Figure 3) with Matlab (The MathWorks, USA) and solve the system of ordinary differential equations with the ode45 routine.

3. RESULTS

3.1 Static response validation

The model should be capable of simulating a variety of basic CVS trends in a physiologically accurate manner. This section investigates the outputs from the closed loop model, comparing results with known physiological trends. It is therefore testing the aggregation of elements tested individually in previous studies.

Figure 4 plots the left and right ventricle pressures and volume evolutions for the closed loop model after it has reached a steady state solution. This plot can be compared with the Wiggers diagram [18]. The model is seen to capture the major dynamics of the CVS including the variations in left ventricle pressure, aortic pressure and ventricle volume.

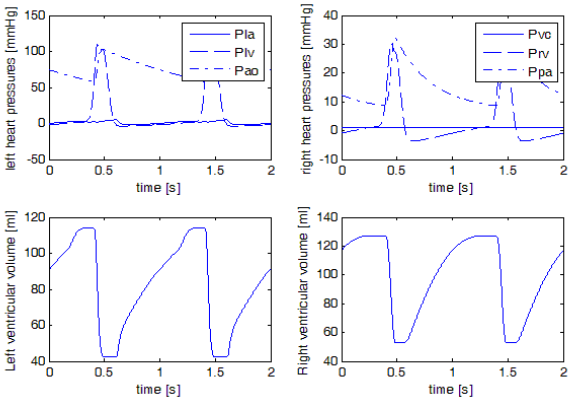

Figure 4 : hemodynamic static response of the simulated CVS model – Pressure evolution in the left and right heart – Volume evolution in the left and right ventricle

The normal motion of the mitral valve during a cardiac cycle has been analyzed by Saito et al. [17]. From this qualitative analysis and quantitative values from literature [19-24], normal mitral aperture evolution as well as transmitral blood flow during the diastole has been reconstructed, regarding the driving pressure. Figure 5 describes the two peaks E-wave and A-wave corresponding respectively to the passive filling of the ventricle and the active one, due to the atrial contraction. Between these two peaks, the driving force of the blood, the pressure difference between both parts of the valve, cancels out. This time period is named diastasis.

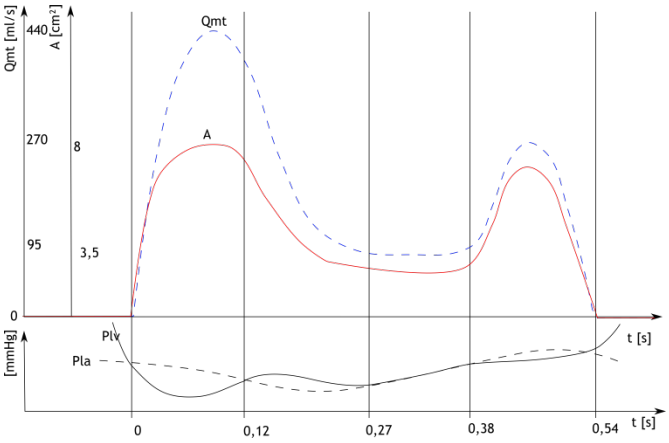

Figure 5 : Physiological evolution of the transmitral blood flow and the mitral valve opening area during the opening period of the mitral valve (HR=60/min)

Figure 6 plots the evolution of the transmitral blood flow as well as the evolution of the mitral valve aperture area. Comparing these plots to Figure 5, the model is seen to capture the complex opening and closing dynamic behavior of the mitral valve with the 3 periods during the opening phase. Although the parameters of the model are adjusted to correspond to a trend and not by fitting the output model signals to a set of data, orders of height, temporal as well as

the values reached by the flow and the area, are globally respected.

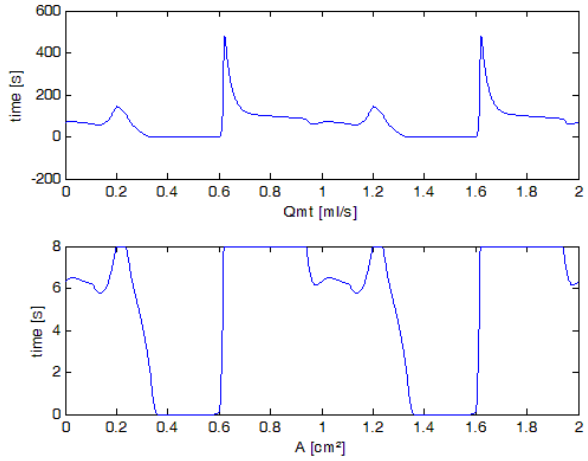

Figure 6 : hemodynamic static response of the simulated CVS model - evolution of the transmitral blood flow - evolution of the mitral valve opening area

Since the ultimate goal is simulation of human heart function, particularly in response to changes in therapy, tests to validate simple trends are carried out comparing model outputs with known physiological trends. Figure 7 shows the effect of varying ventricle contractility, a measure of cardiac pump function [25]. Contractility is varied in the model by changing the end systolic elastance (Ees) [26]. Typically, an increase in contractility results in an increase in cardiac output which correlates with an increase in stroke volume (SV), assuming heart rate remains constant. Figure 7 plots a PV diagram for 3 different contractilities showing the desired increase in stroke volume as contractility increases.

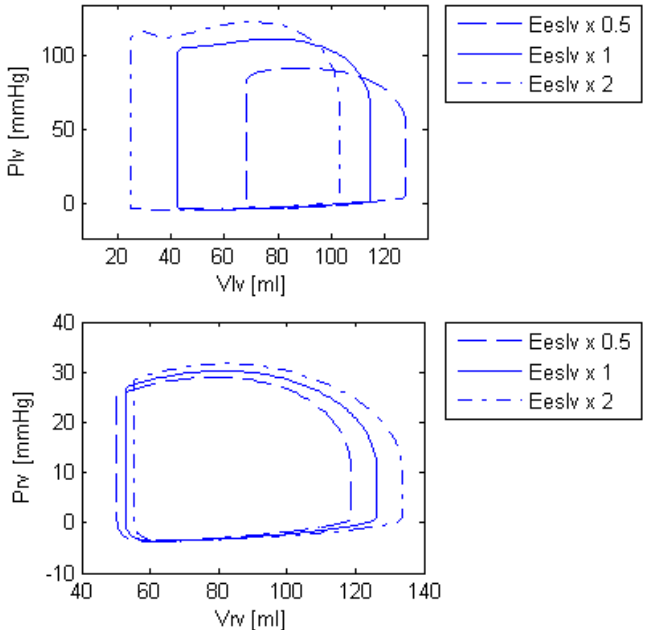

Figure 7 : Effect on left and right pressure-volume loops of changes of contractility

A second test shows the effect of changing the systemic circulatory resistance. Readily available clinical data shows that an acute increase in resistance results in reduced cardiac output that varies with the magnitude of the change [27]. Figure 8 shows the closed loop model output, as systemic resistance is increased, and decreased. As systemic resistance decreases, stroke volume increases, meaning an increase in cardiac output. The opposite trend occurs as the resistance is increased. Figure 9 shows the rise in pressure in the aorta as a result of increased peripheral resistance and the resulting decreased cardiac output (CO), which illustrates the increase in blood pressure (BP) often seen in patients with narrowed or blocked arteries, and the resulting increased systemic resistance. Hence, both figures illustrate that the model captures well-known, basic clinical behavior in response to changes in systemic resistance.

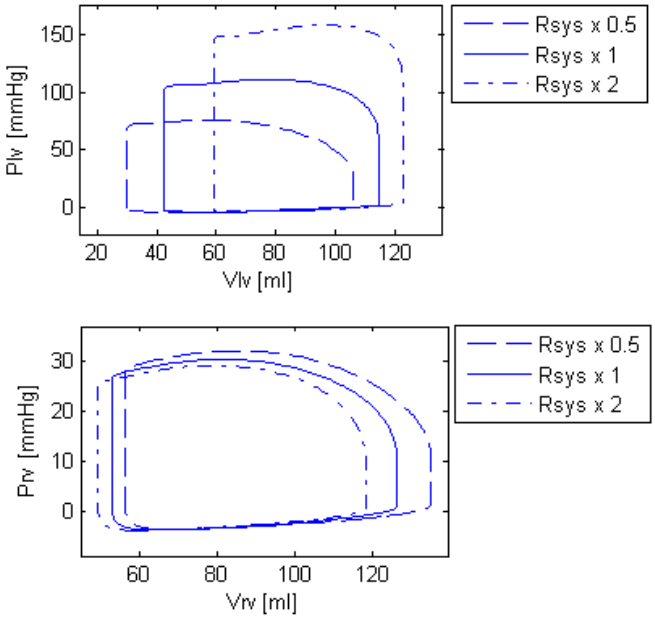

Figure 8 : Effect on left and right pressure-volume loops of changes of the systemic resistance

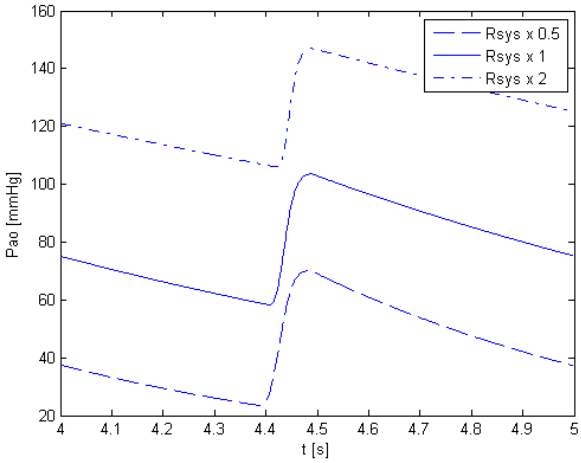

Figure 9 : Response of aortic pressure in response to changes in systemic resistance

Finally, the average thoracic cavity pressure in humans is normally about -2mmHg, however if this pressure is increased, as occurs during positive pressure mechanical ventilation, cardiac output is decreased [18]. As shown in Figure 10, the model is capable of simulating the effect of this common intervention.

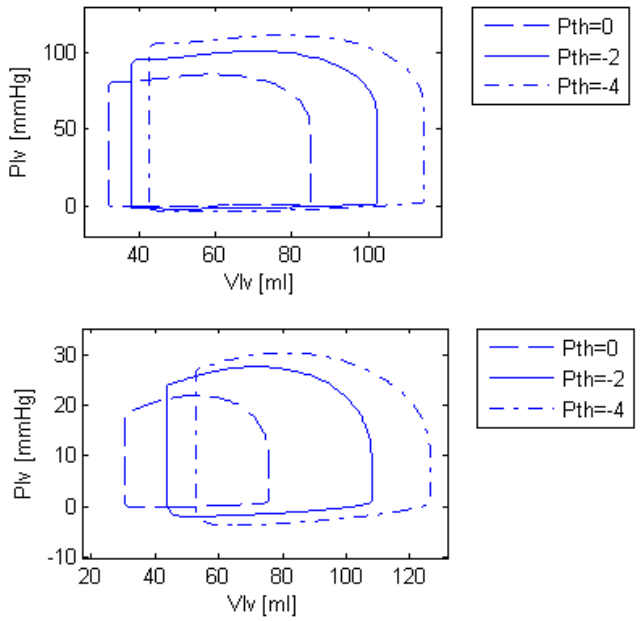

Figure 10 : Change in stroke volume and PV diagram for a change in thoracic pressure

3.2 Dynamic response validation

The minimal CVS model presented has been shown to simulate the static response of the cardiovascular system to changes in state, but the transient dynamic response of the model to these changes has not yet been verified. Tests carried out in section 3.1 show that the static response, or the change in steady state solution, of the model to changes in state matches known physiological response. This section investigates the dynamic response of the CVS system to changes in state, such as arterial constrictions and changes in thoracic pressure due to respiration.

This dynamic response verification focuses on ventricular interactions which are important CVS interactions that contribute significantly to CVS dynamics [28]. Therefore, more understanding of the physiological interactions will improve the capability of medical staff to diagnose and treat CVS dysfunction.

Slinker and Glantz [27] extended earlier studies on ventricular interaction by analysing the transient effects of both direct and series ventricular interaction on CVS dynamics. This research was also carried out on anaesthetized dogs, but the heart remained connected to the circulation system, thus including series interaction between ventricles. This approach takes advantage of the time lag between direct and series interaction when investigating the effect of changing right ventricle state on left ventricle function. Direct interaction, through the septum and pericardium, will cause an immediate response in the left ventricle if the volume of the right ventricle is changed. The changes in left ventricle function due to series interaction will be delayed as the dynamics propagate around the pulmonary circulation. This delay was used to delineate and quantify the relative contributions of series and ventricle interaction to CVS function. However, using the minimal model developed it is possible to directly separate each type of interaction.

The experiment carried out by Slinker and Glantz [27] involved sequentially constricting and releasing the pulmonary artery and vena-cava. Pulmonary artery constriction (PAC) causes an increase in resistance downstream of the right ventricle, increasing the afterload against which the right ventricle must pump. Applying vena-cava constriction (VCC) decreases the pressure upstream of the right ventricle, decreasing the right ventricle preload as a result of reduced filling pressure. When the constrictions are subsequently released the CVS responds again, settling to its original state. These constrictions and their subsequent releases significantly impact the function of the right ventricle. Volumes, pressures and flow rates around both the right and left ventricles were measured to determine the response of the CVS to these changes in state. Very little information about the mechanical properties of the canine hearts studied can be gained from the publication [27]. It is known that the heart rate was maintained at roughly 130 beats per minute, there is no respiration, and the data was taken with the pericardium removed.

To verify that the minimal model captures the experimental dynamics, in spite of the lack of specific information, the model parameters used in section 3.1for the static trend verification are used. The heart rate is changed to 130 beats per minute and the pericardium effects are removed by setting the elastance to a negligible value ($P_{0,pcd} = 10^{-6}$). The pulmonary artery constriction is simulated by increasing the pulmonary valve resistance (Rpv) by a factor of 20. Similarly, the vena-cava constriction is simulated by increasing the tricuspid valve resistance (Rtc) by a factor of 4. These factors for varying the resistances were found by trial and error to approximately match the performance magnitudes of the data in Slinker and Glantz [27].

Primary Experiment and Results

Figure 11 shows the main results obtained by Slinker and Glantz [27]. The experiment shown involved constricting the pulmonary artery after about 4 seconds (PAC) followed by vena-cava constriction after about 12 seconds (VCC). At 20 seconds the constriction on the pulmonary artery is released and after about 27 seconds the vena-cava constriction is released. Figure 11 plots the experimentally determined variations in pressures, volumes and flow rates around both ventricles during these constrictions and releases.

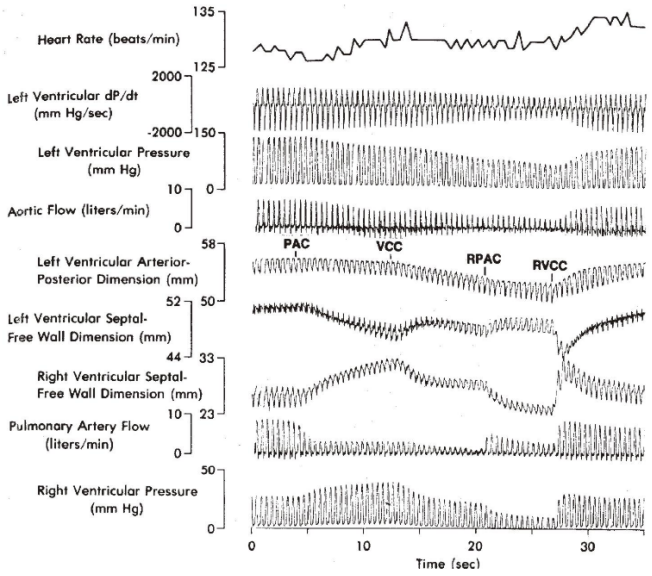

Figure 11 : Hemodynamic CVS responses to sequential constrictions and releases of the pulmonary artery and vena-cava [27]

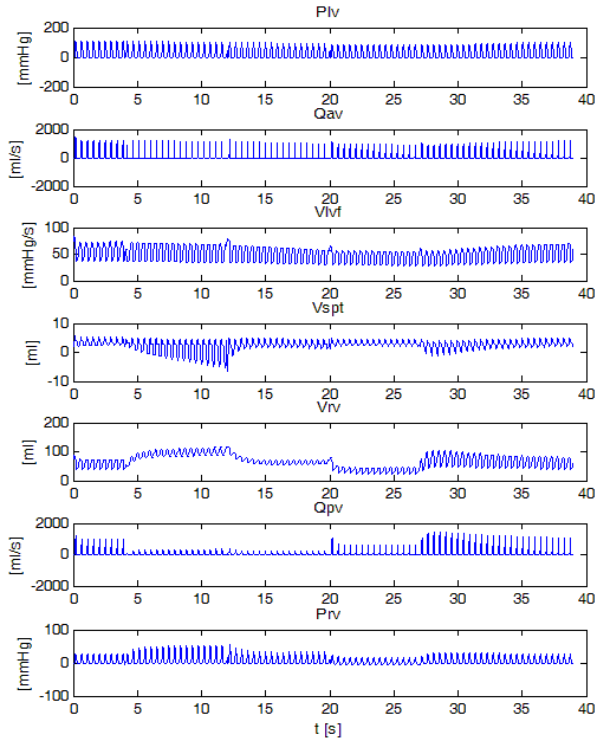

Figure 12 : Hemodynamic CVS responses simulated using the presented model

Figure 12 plots the results of a simulation carried out on the CVS model to simulate the experimental results of Figure 11. Comparing these plots highlights the ability of the CVS model to capture all of the trends measured experimentally [27]. Note that the magnitudes of each variable do not match the experimental results due to the lack of detailed information available and the use of generic human parameters. However, by capturing these trends the model is shown to accurately capture the dynamics of ventricular interaction in the CVS.

Figure 13 plots the variation in left ventricle end-diastolic area, which is assumed to be proportional to left ventricle end-diastolic volume during the experiment. The black dots are experimental data. The solid and dashed lines plot the results of a statistical analysis [27] to capture the changes, and are not experimental data.

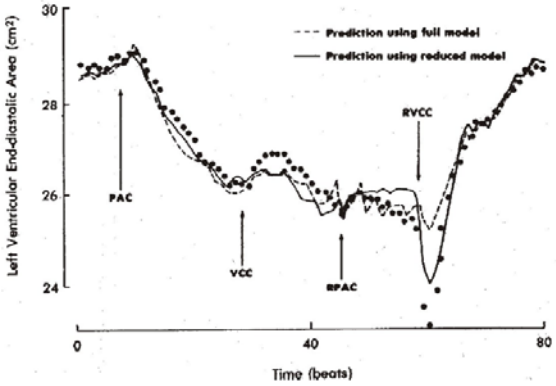

Figure 13 : Experimentally determined change in left ventricle end-diastolic area [27]

Figure 14 plots the variation in simulated left ventricle volume (V_{lv}) using the CVS minimal model.

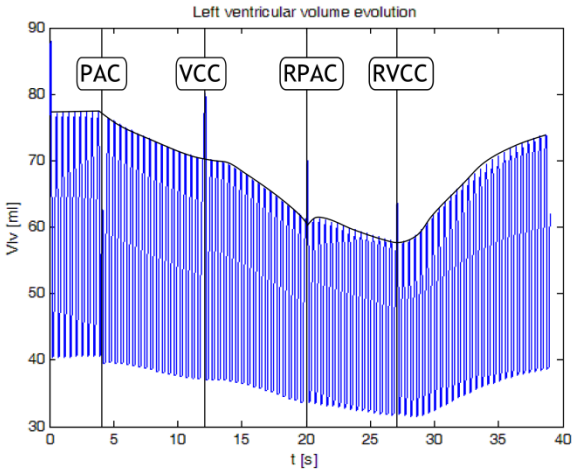

Figure 14 : Simulated variations in left ventricle volume (blue) and end diastolic volume (black line)

Second Experiment and Results

A second experiment involved applying a different combination of the same constrictions [27]. The pulmonary artery constriction is again applied after 4 seconds, but released after about 23 seconds. At about 37 seconds a subsequent vena-cava constriction is applied until the end of the experiment.

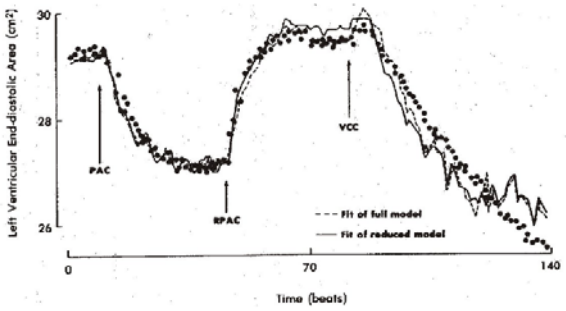

Figure 15 : Hemodynamic CVS responses to sequential constrictions and releases of the pulmonary artery and vena-cava [27]

The experimentally measured variations in left ventricle end-diastolic area are plotted in Figure 15. This experiment was also simulated using the minimal model, and the trends shown in Figure 16 are seen to accurately match experimental results.

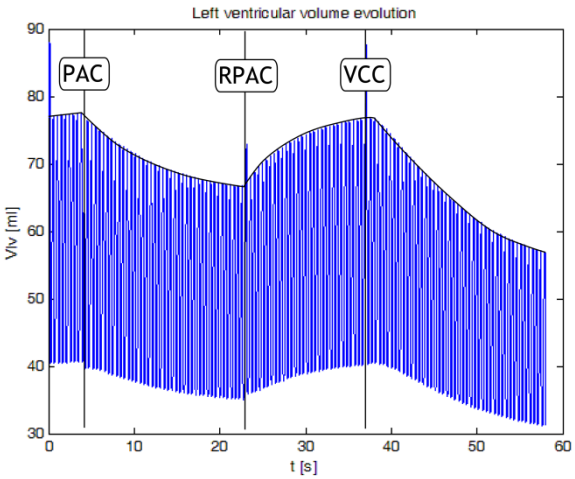

Figure 16 : Simulated variations in left ventricle volume (blue) and end diastolic volume (black line)

4. CONCLUSIONS

This work describes a new closed-loop model of the cardiovascular system that accounts for progressive mitral valve aperture. Simulations show good correlation with physiologically expected results for healthy valves in static and dynamic simulations. The large number of valve model parameters indicates a need for emerging, lighter and minimal mitral valve models that are readily identifiable to achieve full benefit in real-time use. These results suggest a further use of this model to track, diagnose and control valves pathologies.

5. REFERENCES

1. Burkhoff, D., J. Alexander, and J. Schipke, *Assessment of Windkessel as a Model of Aortic Input Impedance.* American Journal of Physiology, 1988. **255**(4): p. H742-H753.
2. Shim, E.B., et al., *A new integrated method for analyzing heart mechanics using a cell-hemodynamics-autonomic nerve control coupled model of the cardiovascular system.* Progress in Biophysics and Molecular Biology, 2008. **96**(1-3): p. 44-59.
3. Kerckhoffs, R.C.P., et al., *Coupling of a 3D finite element model of cardiac ventricular mechanics to lumped systems models of the systemic and pulmonic circulation.* Annals of Biomedical Engineering, 2007. **35**(1): p. 1-18.
4. Hunter, P.J., et al., *An Anatomical Heart Model with Applications to Myocardial Activation and Ventricular Mechanics.* Critical Reviews in Biomedical Engineering, 1992. **20**(5-6): p. 403-426.
5. Smith, B.W., et al., *Minimal haemodynamic system model including ventricular interaction and valve dynamics.* Medical Engineering and Physics, 2004. **26**(2): p. 131-9.
6. Hann, C.E., J.G. Chase, and G.M. Shaw, *Efficient implementation of non-linear valve law and ventricular interaction dynamics in the minimal cardiac model.* Computer Methods and Programs in Biomedicine, 2005. **80**(1): p. 65-74.
7. Olansen, J.B., et al., *A closed-loop model of the canine cardiovascular system that includes ventricular interaction.* Computers and Biomedical Research, 2000. **33**(4): p. 260-95.
8. Desaive, T., et al., *Cardiovascular Modelling and Identification in Septic Shock - Experimental validation.* Proceedings of the 17th IFAC World Congress July 6-11, 2008, Seoul, Korea, 2008: p. 2976-9.
9. Desaive, T., et al., *Study of ventricular interaction during pulmonary embolism using clinical identification in a minimum cardiovascular system model.* Conf Proc IEEE Eng Med Biol Soc, 2007. **2007**: p. 2976-9.
10. Paeme, S., et al., *Mathematical multi-scale model of the cardiovascular system including mitral valve dynamics. Application to ischemic mitral insufficiency.* Biomed Eng Online, 2011. **10**(1): p. 86.
11. Paeme, S., et al. *Mathematical model of the mitral valve and the cardiovascular system : application for studying and monitoring valvular pathologies*. in *UKACC International Conference on CONTROL 2010*. 2010. Coventry.
12. Moorhead, K.T., et al., *A simplified model for mitral valve dynamics.* Computer Methods and Programs in Biomedicine, 2011.
13. Smith, B.W., et al., *Experimentally verified minimal cardiovascular system model for rapid diagnostic assistance.* Control Engineering Practice, 2005. **13**(9): p. 1183-1193.
14. Starfinger, C., et al., *Model-based cardiac diagnosis of pulmonary embolism.* Computer Methods and Programs in Biomedicine, 2007. **87**(1): p. 46-60.

15. Starfinger, C., et al., *Model-based identification of PEEP titrations during different volemic levels.* Computer Methods and Programs in Biomedicine, 2008. **91**(2): p. 135-144.
16. Starfinger, C., et al., *Model-based identification and diagnosis of a porcine model of induced endotoxic shock with hemofiltration.* Mathematical Biosciences, 2008. **216**(2): p. 132-9.
17. Saito, S., et al., *Mitral valve motion assessed by high-speed video camera in isolated swine heart.* Eur J Cardiothorac Surg, 2006. **30**(4): p. 584-91.
18. Guyton, A.C., *Textbook of medical physiology*. 1991, Philadelphia: Saunders.
19. Mynard, J.P., et al., *A simple, versatile valve model for use in lumped parameter and one-dimensional cardiovascular models.* International Journal for Numerical Methods in Biomedical Engineering, 2011: p. n/a-n/a.
20. Szabó, G., et al., *A new computer model of mitral valve hemodynamics during ventricular filling.* European Journal of Cardio-Thoracic Surgery, 2004. **26**(2): p. 239-247.
21. Flewitt, J.A., et al., *Wave intensity analysis of left ventricular filling: application of windkessel theory.* Am J Physiol Heart Circ Physiol, 2007. **292**(6): p. H2817-23.
22. Bowman, A.W., P.A. Frihauf, and S.J. Kovacs, *Time-varying effective mitral valve area: prediction and validation using cardiac MRI and Doppler echocardiography in normal subjects.* Am J Physiol Heart Circ Physiol, 2004. **287**(4): p. H1650-7.
23. Courtois, M., S.J. Kovacs, Jr., and P.A. Ludbrook, *Transmitral pressure-flow velocity relation. Importance of regional pressure gradients in the left ventricle during diastole.* Circulation, 1988. **78**(3): p. 661-71.
24. Nelson, M.D., et al., *Increased left ventricular twist, untwisting rates, and suction maintain global diastolic function during passive heat stress in humans.* Am J Physiol Heart Circ Physiol, 2010. **298**(3): p. H930-7.
25. Kass, D.A. and W.L. Maughan, *From 'Emax' to pressure-volume relations: a broader view.* Circulation, 1988. **77**(6): p. 1203-12.
26. Burkhoff, D. and J.V. Tyberg, *Why does pulmonary venous pressure rise after onset of LV dysfunction: a theoretical analysis.* American Journal of Physiology, 1993. **265**(5 Pt 2): p. H1819-28.
27. Slinker, B.K. and S.A. Glantz, *Beat-to-beat regulation of left ventricular function in the intact cardiovascular system.* American Journal of Physiology, 1989. **256**(4 Pt 2): p. R962-75.
28. Weber, K.T., et al., *The contractile behavior of the heart and its functional coupling to the circulation.* Progress in Cardiovascular Diseases, 1982. **24**(5): p. 375-400.